Influence of the Interactions in Aqueous Mixtures of Poly(vinyl methyl ether) on the Crystallization Behavior of Water

Jianming Zhang,[†] Bert Bergé,[‡] Frank Meeussen,[‡] Erik Nies,[‡,§] Hugo Berghmans,[*,‡] and Deyan Shen[*,†]

State Key Laboratory of Polymer Physics & Chemistry, Center for Molecular Science, Institute of Chemistry, 506 Group, Chinese Academy of Sciences, Zhongguancun, Beijing 100080, Peoples' Republic of China; Polymer Research Division, Department of Chemistry, Catholic University of Leuven, Celestijnenlaan 200F, B-3001 Heverlee, Belgium; and Laboratory of Polymer Technology, Eindhoven University of Technology, P.O. Box 513, 5600MB Eindhoven, The Netherlands

Received July 14, 2003

ABSTRACT: Aqueous solutions of poly(vinyl methyl ether) are experimentally studied at temperatures below the equilibrium freezing temperature of water. Earlier investigations of the peculiar phase behavior of PVME/water gave evidence of the existence of a molecular solvent/polymer complex in which (at most) two water molecules per repeating unit are hydrogen bonded to the polymer chain. In favor of the complex formation hypothesis is the abrupt arresting of the crystallization and melting of water in mixture with $w_{PVME} > 0.61$. To relate this peculiar crystallization behavior and complex formation to the thermal and kinetic stability of the complex, the crystallization of water is explored in detail using thermal, volumetric, spectroscopic, X-ray scattering techniques, and morphological investigations. Our results clearly indicate the significant influence of the experimental conditions on the crystallization and subsequent melting of water. In agreement with previous results and for certain experimental conditions used in this study, the existence of a molecular complex is confirmed. However, additional experiments demonstrate that the complex is thermodynamically unstable and is only observed under certain kinetic conditions. For polymer concentrations $w_{PVME} < 0.61$ (almost) full crystallization of water can be realized by isothermal annealing in the temperature region −20 to −30 °C or slow cooling to low temperature. Furthermore, also in the concentration range $w_{PVME} > 0.61$ the crystallization of water can be realized provided the nucleation of water is facilitated. It is anticipated that the crystallization under previously employed crystallization conditions does not occur because the activation energy for nucleation is too large under the experimental conditions, and it is the nucleation that is arrested.

1. Introduction

Aqueous polymer solutions have already received considerable research interest from academic and practical points of view.[1,2] Water-soluble polymers find numerous use in for example food and or pharmaceutical applications. The academic interest is at least in part triggered by the often peculiar and complicated behavior shown by aqueous polymer solutions. In hindsight, the peculiar behavior often turns out to be essential for the practical applications. For instance, the large changes in volume encountered when aqueous polymer gels change from a swollen to a collapsed state or vice versa with small changes in external parameters such as temperature or pH are well documented for gels of poly(*N*-isopropylacrylamide) (PNIPA).[3,4] Also, gels of poly(vinyl methyl ether) (PVME), obtained after cross-linking the linear polymer with γ-irradiation show abrupt changes in swelling behavior with temperature.[5] For these polymer gels it has been demonstrated that the volume transition can be traced back to the unusual lower critical solution temperature (LCST) miscibility behavior of the corresponding linear polymers in water.[6−9] The most striking observation is the existence of a liquid−liquid LCST critical condition at high polymer concentrations that practically does not change with molar mass, yielding—in the limit of infinite chain length—a nonzero limiting critical concentration.[7] This is in discrepancy with the predictions derived from Flory−Huggins theory dominating our understanding of polymer solution phase behavior for decades now.[10,11] This nonzero limiting concentration can be the only critical state in the systems, as it is the case for poly(*N*-isopropylacrylamide) in water,[4] or it can be one of two stable critical points on a bimodal LCST. This is the case in for example PVME in water.[8] The second stable critical point is governed by the combinatorial entropy contribution to the Gibbs energy and behaves as expected from Flory−Huggins theory.

Apart from the high-temperature phase behavior, aqueous polymer solutions also have been investigated at temperatures below the normal freezing point of water. A frequently investigated polymer in this respect is poly(vinylpyrrolidone) (PVP).[12] Depending on the concentration and temperature regimes, different types of irregular ice crystallization patterns have been observed. Similar observations have been made already in water/glycerol mixtures.[12] Additionally, in the case of PVP the melting point of water in the mixture was found to decrease sharply in the vicinity of $w_{PVP} \sim 0.6$, beyond which water no longer could be crystallized.[13] Such highly concentrated solutions are very viscous and remain homogeneous solutions and eventually vitrify at sufficiently low temperatures. The water in these non-crystallizable solutions is assumed to be bound to the polymer chain. Whether this is kinetically or thermodynamically controlled is not completely clear, and the matter is far from solved as a more recent study of

[†] Chinese Academy of Sciences.
[‡] Catholic University of Leuven.
[§] Eindhoven University of Technology.
* Corresponding authors: e-mail Hugo.Berghmans@chem.kuleuven.ac.be; Dyshen@pplas.icas.ac.cn.

10.1021/ma0303869 CCC: $25.00
Published on Web 10/30/2003

highly concentrated PVP/water mixtures demonstrates. Employing time-resolved SAXS measurements, transient columnar structures forming a plane hexagonal lattice in the highly concentrated mixtures have been found to exist, which become noticeable in the 2-dimensional SAXS scattering pattern as intense but short-lived spots.[14] It was suggested that these structures are induced by the formation of liquid-crystalline structures in PVP. Moreover, the scattering spectra were found to increase over time, the more pronounced at lower temperatures.[15] From these data it was concluded that the systems at high concentrations are not in equilibrium but are in a state of slowly progressing liquid−solid phase separation. From these data a new estimate of the location of the equilibrium melting line of water was given and suggested not to decrease as sharply as assumed in the earlier investigations. The high glass transition temperature of PVP makes that highly viscous mixtures are obtained which at low temperature are prone to vitrification. Consequently, experimental and characteristic time scales in the system become comparable, and nonequilibrium conditions persisting over extended periods of time may erroneously be viewed as an equilibrium state.

In this paper the crystallization behavior of water in aqueous PVME solutions is investigated over the complete concentration range. In PVME/water similar observations as in PVP/water have been made concerning the peculiar crystallization behavior as well as the existence of transient SAXS scattering peaks.[16] However in contrast to PVP, PVME is assumed to be sufficiently flexible and most likely has no liquid-crystalline state. Depending on the crystallization temperature and the concentration, different modes of ice crystallization have been observed,[16] in agreement with the results found in PVP/water and glycerol/water mixtures.[12] Also in agreement with the PVP/water results, it has been observed that the crystallization of water in PVME/water is arrested at polymer concentrations higher than $w_{PMVE} \sim 0.61$.[17] However, in this case, the interference with T_g is not a problem as the glass transition temperatures is located at −19 °C and a lower T_g is observed in the polymer solutions anyway. (The T_g of a polymer solution containing $w_{PVME} = 0.61$ is ca. −60 °C, and the melting temperature is ca. −20 °C.) Apart from the similarities with other aqueous polymer systems, PVME/water is also characterized by further peculiarities. For instance, the glass transition temperature as a function of temperature is not a smoothly varying function of composition but shows a change in course with composition at again $w_{PVME} = 0.61$.[17] In the case of PVME/water all this information was assumed to point to the formation of a molecular solvent/polymer complex in which (at most) two water molecules per repeating unit are hydrogen bonded to the polymer chain.

Changes in hydrogen bonding between water molecules and the repeating unit of a series of polymers, including PVP and PVME, can clearly be followed by FTIR measurements.[18−20] Interesting information on the crystallization of water in the presence of PVME was already obtained on the influence of temperature and concentration on the specific IR absorptions.[21,22] The site-specific IR information has been interpreted to show the existence of different levels of hydration and/or complexation of the polymer chain. For instance, below −34 °C the PVME/water complex obtained from a 50 wt % PVME aqueous solution seems to be stable. Changes in the spectrum during a subsequent heating of the samples to higher temperature indicate the crystallization and subsequent melting of water. This phenomenon has been observed earlier for other aqueous polymer solutions.[23]

However, as illustrated in this Introduction, the crystallization of any component involves kinetic aspects. To relate the peculiar crystallization behavior in general and the complex formation in particular to the thermal and kinetic stability of the complex, quantitative information on the crystallization of water is necessary. This aspect will be investigated in detail in this paper and will be approached through the investigation of the crystallization and melting of water, in combination with spectroscopic, volumetric, and morphological investigations.

2. Experimental Details

2.1. Materials. PVME was purchased from Aldrich. The number-average and mass-average molar masses and the molar mass distribution were determined by GPC in THF using polystyrene as the calibration standard. This determination resulted in a mass average $M_w = 20$ kg/mol and a number-average $M_n = 10$ kg/mol, leading to a polydispersity index $M_w/M_n = 2$.

Distilled water was used. All components were used without further purification. Concentrations are expressed in mass fraction, w_i, of each component i.

PVME solutions were allowed to homogenize at room temperature for periods up to 2 months for the highest polymer concentrations.

2.2. Techniques. Calorimetry. A Perkin-Elmer DSC7 was used for the calorimetric observations. The thermal treatment of the sample and the scanning rates are given in the text.

FTIR Spectroscopy. All spectra were recorded on Bruker EQUINOX 55 spectrometer and processed by the Bruker OPUS program. A sample solution was put between two CaF_2 windows without spacer, and the sample thickness was adjusted to make the maximum absorbance of target IR bands smaller than 2 absorbance units. The background spectrum for one cycle of the measurement was obtained with a clear CaF_2 window. The spectra were obtained by averaging 32 scans at a 2 cm^{-1} resolution. A Bruker P/N 21525 series variable temperature cell was used.

Optical Microscopy. Optical microscopy observations were performed using an Olympus BH-2 microscope equipped with a Mettler heating−cooling stage. Liquid nitrogen was used for cooling the samples in the low-temperature region.

X-ray Scattering. Time-resolved SAXS/WAXS experiments were carried out at the Dutch-Belgian Beamline (DUBBLE-CRG, ESRF, Grenoble, France). The SAXS/WAXS data were recorded simultaneously with a quadrant[24] and a curved linear detector[25] at a wavelength 1.24 Å. The time resolution between patterns during heating was 1 min, corresponding to temperature resolution of 1 °C. Isothermal crystallization of linear polyethylene data were collected every second. The WAXS and SAXS patterns were corrected for the detector response and normalized to the intensity of the primary beam measured by an ionization chamber placed upstream from the sample. The latter procedure corrects for changes in the intensity of the incoming beam and accounts for changes in sample transmission. The scattering vector axis of the SAXS region was calibrated using the first nine orders of dry calcified collagen, and the 110 and 200 reflections of a quenched linear polyethylene were used to calibrate the WAXS axis.

3. Results

3.1. Calorimetric Results. 3.1.1. Calorimetric Quantification of the Melting of Water. Based on previous results, the crystallization of water was investigated over the whole polymer concentration range. The

Table 1. Melting Enthalpies of Samples Quenched to −40 °C and Heated at 1 °C/min

w_{PVME}	ΔH_{melt}, J/g solution
0.10	271.5
0.30	170.5
0.40	116.6
0.60	55.6

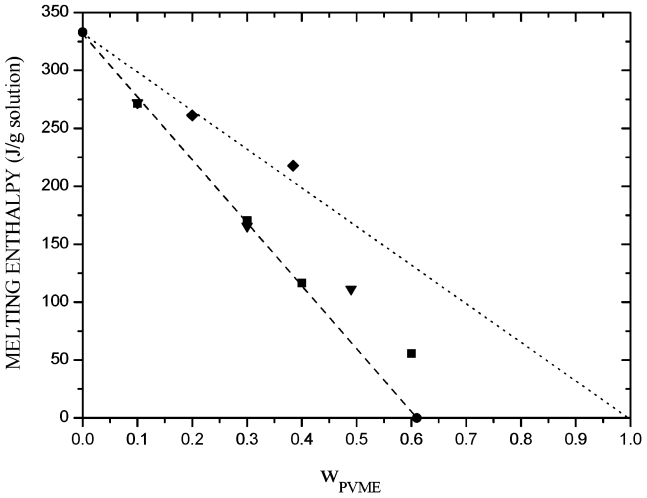

Figure 1. Concentration dependence of the melting enthalpy of water for the system PVME/water, crystallized under different experimental conditions: (■) quenching to −40 °C, heating at 1 °C/min; (◆) cooling to − 60 °C at 1 °C/min, heating at 1 °C/min; (▼) fast cooling to −50 °C, 11 days isothermal, heating 10 °C/min; (●) ice and composition of complex.

Table 2. Melting Enthalpy as a Function of Concentration after Isothermal Crystallization at −50 °C for 11 days

w_{PVME}	ΔH_{melt}, J/g solution
0.104	272.2
0.304	165.6
0.486	111.4

data reported in a previous paper were the result of dynamic experiments performed in the DSC.[17] In these experiments the samples were subjected to a cooling−heating cycle at 2 °C/min. In view of the serious kinetic problems that can be encountered in such measurements and to investigate the influence of the kinetics of the water crystallization process on the melting behavior, different thermal treatments are applied in the current investigation.

In the lower concentration range, i.e., $w_{PVME} < 0.61$, data on the melting of water were easily obtained after the application of different thermal treatments. For the thermal treatment conditions discussed in this section no crystallization of water was observed when $w_{PVME} > 0.61$.

Crystallization Observed after Quenching and during Slow Heating at 1 °C/min. Samples of different polymer concentration were quenched to −40 °C and then immediately heated at 1 °C/min. The resulting melting enthalpies are reported in Table 1 and plotted in Figure 1.

Isothermal Crystallization at −50 °C. Samples with different polymer content were quenched to and isothermally crystallized at −50 °C for 11 days. In this case the DSC scanning rate used during heating is 10 °C/min. The resulting melting enthalpies are reported in Table 2 and plotted in Figure 1.

Table 3. Melting Enthalpy as a Function of Concentration after Slow Cooling

w_{PVME}	ΔH_{crys}, J/g solution	ΔH_{melt}, J/g solution
0.20	288.6	261.3
0.384	194.9	217.7

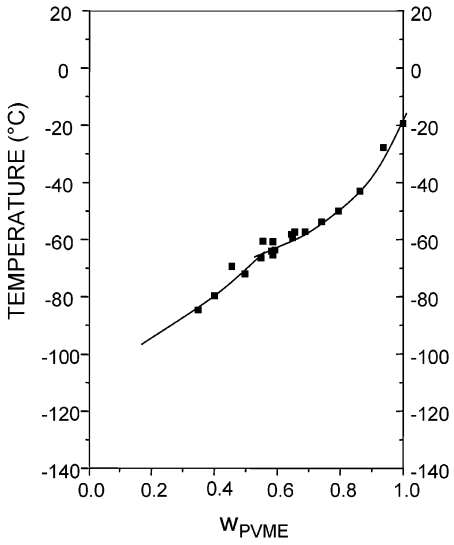

Figure 2. Glass transition−composition curve for the system PVME/water.

Crystallization during Slow Cooling. Samples with different polymer concentrations were cooled at 1 °C/min to −60 °C, kept at this temperature for 60 min, and then heated at 1 °C/min. The DSC scans were recorded during cooling and heating, and the corresponding crystallization and melting enthalpies (ΔH_{crys} and ΔH_{melt}) were recorded. They are reported in Table 3, and the data are plotted in Figure 1.

The values in both columns are, within the experimental accuracy, quite similar so that we can conclude that the crystallization of water is already almost complete at the end of the cooling scan.

3.1.2. Calorimetric Quantification of the Glass Transition Temperature. The glass transition temperature−concentration relation was already reported in a previous paper and is presented in Figure 2 for later discussion.[17] These T_g data were obtained after quenching the samples in liquid nitrogen so that crystallization of water could be avoided. The lowest polymer concentration for which the crystallization of water was still prevented was $w_{PVME} = 0.35$.

Glass Transition Temperatures after Crystallization. Figure 3 shows the DSC curve of a solution with $w_{PVME} = 0.50$ that was annealed at −30 °C for the indicated periods of time. The sample is cooled from 25 to −30 °C with a cooling rate of 10 °C/min and kept at −30 °C for 0 (a), 30 (b), and 60 min (c). At the end of this annealing period the sample is quickly brought to −70 °C and then heated to 25 °C with 10 °C/min. During cooling at 10 °C/min to −30 °C (almost) no crystallization takes place. The following observations can be made during the subsequent heating run:

When no annealing is performed at this low temperature, crystallization of water, followed by the melting of ice, mainly takes place on heating.

An increase of the annealing time at −30 °C results in more crystallization during the annealing and less crystallization during the subsequent heating process in the DSC experiment. After 30 min only a small

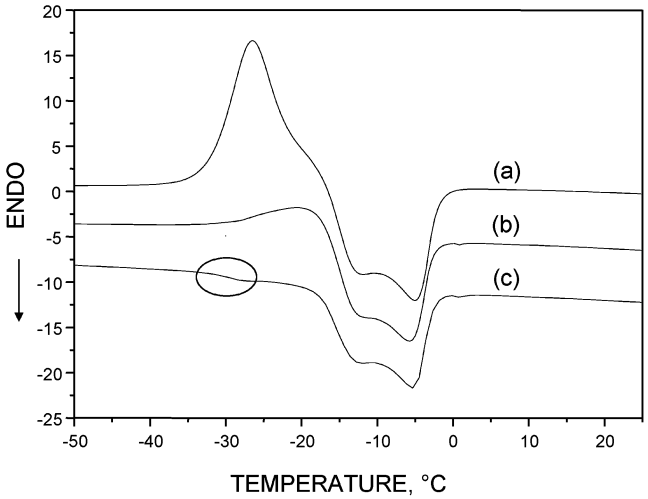

Figure 3. DSC scans of the melting of ice in PVME solutions after annealing at −30 °C ($w_{PVME} = 0.50$) for different times: (a) 0, (b) 30, and (c) 60 min.

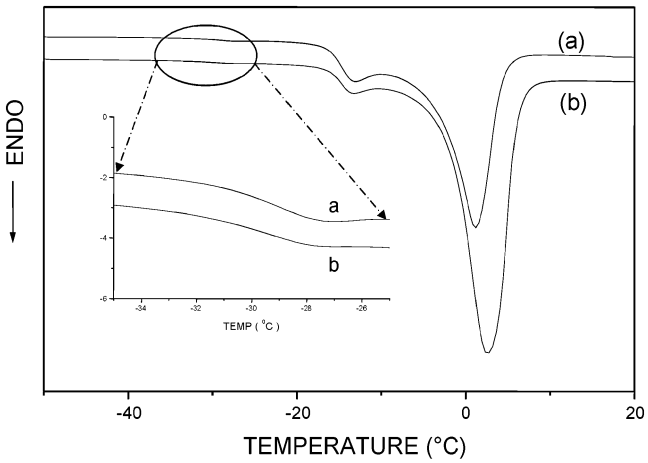

Figure 4. DSC scans of the melting of ice in PVME solutions after annealing at −30 °C for 60 min: (a) $w_{PVME} = 0.20$; (b) $w_{PVME} = 0.30$.

amount of ice is formed during heating, which is seen by the small exothermic signal during the heating while the melting peak is similar to the one observed in the previous experiment.

After 60 min annealing, the exothermic peak has completely disappeared. Meanwhile, a glass transition can be observed around −30 °C (encircled part of the scan). This observation supports the idea that annealing leads to complete crystallization of water with decomposition of the molecular complex. The $T_g = -30$ °C suggests that a small fraction (around 0.06) of water is still present in the polymer. This can be understood by the fact that during this crystallization the sample comes close to its T_g so that complete crystallization of water becomes almost impossible. Consequently, the system has separated into ice and a glassy phase with $w_{PVME} \approx 0.94$.

Normally, this separation into ice and a vitrified concentrated polymer solution should proceed for any polymer concentration up to the concentration where the T_g of the polymer solution equals the annealing temperature. For lower polymer concentrations this is indeed observed and is illustrated in Figure 4 for two different polymer concentrations, i.e., $w_{PVME} = 0.20$ and 0.30.

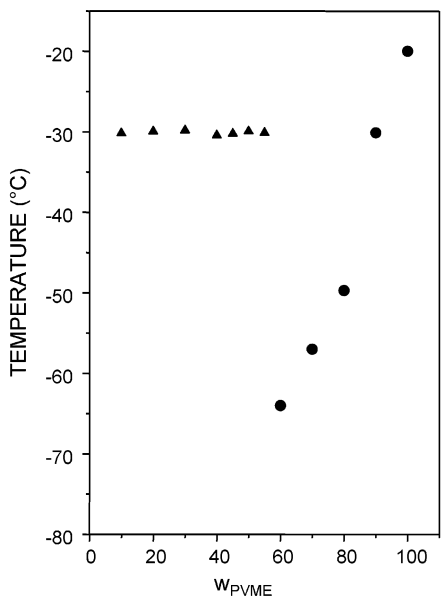

Figure 5. Glass transition as a function of polymer content after annealing at −30 °C.

The part of the scan that shows the glass transition has been enlarged and inserted in the figure. However, for higher polymer concentrations the situation is somewhat different. When the glass transition is plotted as a function of polymer content, two different regimes can be observed (Figure 5). A constant T_g at −30 °C is observed for $0 < w_{PVME} < 0.61$. This clearly illustrates that, in this concentration range and for the crystallization conditions used, the crystallization of water occurs until the system PVME/water reaches its glass transition temperature at −30 °C, corresponding with $w_{PVME} \approx 0.94$. For concentrations higher than $w_{PVME} > 0.61$ the crystallization of water does not occur and the solution vitrifies upon cooling, giving a glass transition temperature that decreases with increasing water content as expected for homogeneous solutions or mixtures.

3.2. Dilatometry. Volume−Temperature Measurements. To avoid the interference with kinetic aspects of crystallization, dilatometry was chosen as an alternative method to investigate the melting of ice under equilibrium conditions.

A typical volume−temperature recording is represented in Figure 6 for a solution with $w_{PVME} = 0.10$. Equilibrium conditions are realized through the specific temperature program that is applied. The dilatometer is placed in the thermostat at room temperature. The cooling is then switched on, and the system approaches the set temperature (−40 °C in this case) very slowly, especially at the end of the process. The whole process takes about 6 h. The system is kept at this low temperature for about 60 h, and then heating is started to a certain temperature. Each data point at a certain temperature in Figure 6 is the result of three consecutive measurements giving the same volume reading. The whole procedure to take the equilibrium readings takes about 100 h. For the example in Figure 6 it can be observed that melting sets in around −21 °C (T_{on}) and ends at 0 °C (T_m). Hence, for this polymer concentration, $w_{PVME} = 0.10$, no melting point depression of water can be observed within experimental accuracy. The same procedure was applied for $w_{PVME} = 0.20$ and 0.50. The data are collected in Table 4.

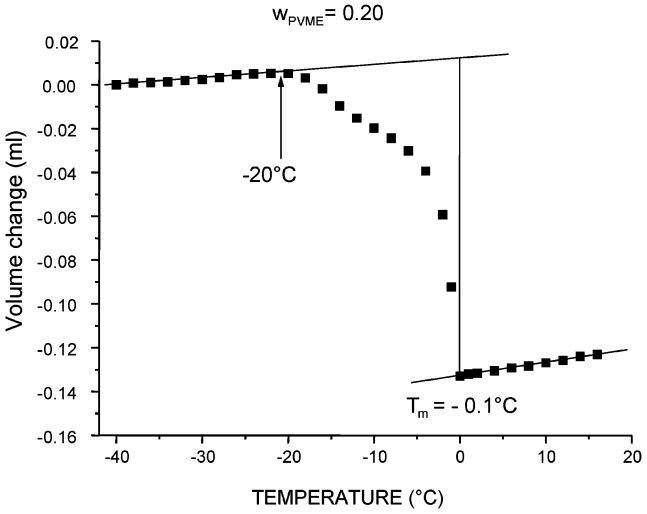

Figure 6. Volume−temperature relation obtained by the dilatometric observation of the melting of ice ($w_{PVME} = 0.20$).

Table 4. Dilatometric Observation of the Onset of Melting and Final Melting Point as Function of Polymer Content

w_{PVME}	T_{on} (°C)	T_m (°C)
0.10	−21	0.0
0.20	−20	−0.1
0.50	−33	−6.1
>0.61		

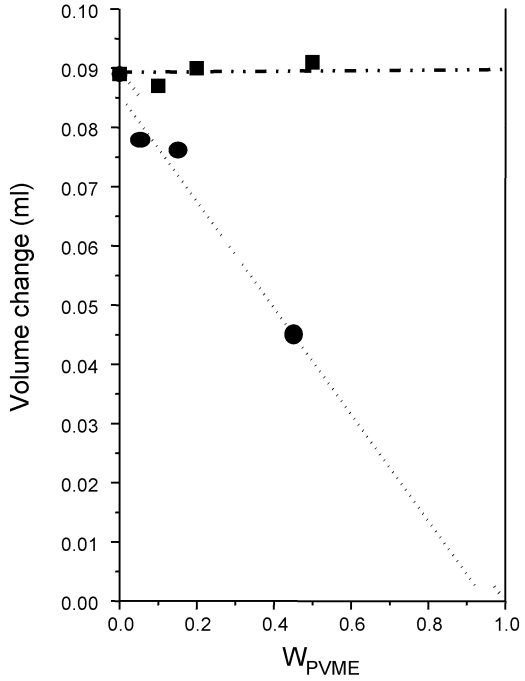

Figure 7. Polymer concentration dependence of the volume change during the melting of ice in solution with different polymer content: (●) volume change per gram of water; (■) volume change per gram solution.

The change in volume per gram of solution is reported in Figure 7 and decreases linearly and extrapolates to zero at $w_{PVME} = 1.00$. This indicates that all water present crystallizes during these experiments. Such a result is to be expected from the calorimetric data reported earlier. During slow cooling, which is also applied in these experiments, complete crystallization takes place already during cooling. Indeed, at temperatures around −20 °C crystallization of water will lead

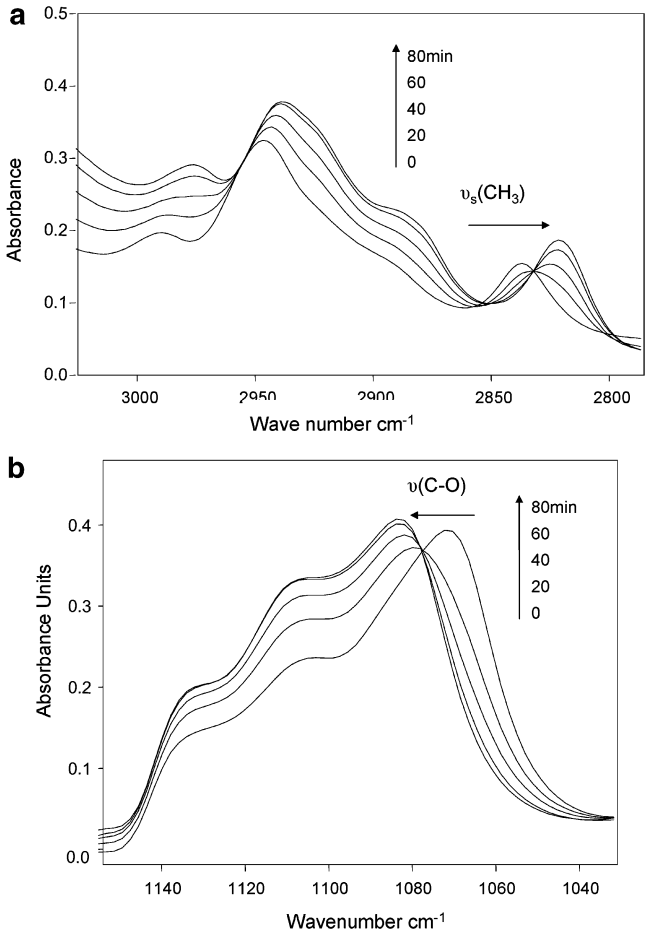

Figure 8. Time evolution with time of IR spectra of PVME in aqueous solution during isothermal annealing at −30 °C in the region of 3000−2800 cm^{-1} (a) and in the 1200−1000 cm^{-1} (b).

to almost pure PVME ($T_g = -19$ °C). An important observation however is the absence of crystallization of water at $w_{PVME} > 0.61$, in agreement with the results obtained from DSC experiments.

3.3. Spectroscopic Analysis. FTIR spectra can provide site-specific molecular information between water and polymer. Figure 8 shows for a solution with $w_{PVME} = 0.50$ annealed at −30 °C the evolution with time of the IR spectrum in the region of the C−H stretching bands and C−O stretching bands. A red shift of the $\nu(CH_3)$ (Figure 8a) and blue shift of the ν(C−O) (Figure 8b) are observed. The occurrence of such shifts was already reported by Maeda[19] when investigating the phase transition in solutions of PVME in D_2O around 35 °C, i.e., the two-phase region. These changes in hydration can be ascribed to changes in the concentration in solution. Similar shifts are observed in our spectra obtained with samples annealed at −30 °C, pointing to a change in the environment of the PVME polymer chains as a consequence of the crystallization of water. These IR observations are in line with the DSC annealing experiments where the crystallization of water is also observed as a function of time and practically finished after 60 min. Also in the IR spectra due to the crystallization of water the PVME environment becomes richer in PVME, in agreement with the red shifts of the $\nu(CH_3)$ (Figure 8a) and blue shifts of the ν(C−O). The shifts are practically complete after 60 min. Hence, IR is an elegant technique to observe the

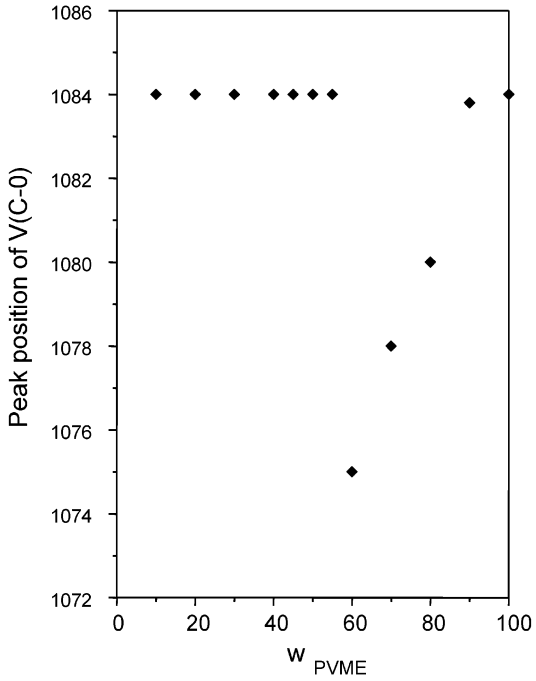

Figure 9. Change in peak position ν(C−O) as a function of PVME concentration after annealing at −30 °C. The samples with w_{PVME} between 0.40 and 0.60 are annealed for a long enough time to complete crystallization of water. Temperature of the measurement is −50 °C.

changes in concentration in situ during annealing experiments.

The peak position of the ν(C−O) band as a function of concentration is plotted as a function of PVME concentration in Figure 9. The samples were annealed at −30 °C for a sufficiently long time so that crystallization is complete and no further shift in the ν(C−O) peak position is observed. The samples were then cooled to −50 °C, and the ν(C−O) peak position is then determined. In the concentration range $0.61 < w_{PVME} < 1.00$ water is unable to crystallize, and the frequency continuously shifts to lower values, in agreement with a changing environment of the PVME polymer chains with solution composition. It should be noted that this shift is not a linear change with composition; down to $w_{PVME} \sim 0.9$ the peak shift is very small and then increases for larger water concentrations. In the concentration region $w_{PVME} < 0.61$, the frequency is very close to what is observed for pure PVME, although from the experimental results the concentration is also in agreement with a concentration of $w \sim 0.96$, in agreement with the observations from crystallization experiments described in sections 3.1 and 3.2.

Comparison of Figures 9 and 5 indicates that the DSC and IR observations are in close agreement, giving consistent evidence for the full crystallization of water under the crystallization conditions applied.

3.4. Morphological Observations. The data reported in the previous paragraphs clearly show the influence of the experimental conditions on the crystallization of water. Additional information concerning this crystallization is obtained from morphological observations by optical microscopy in combination with X-ray scattering.

3.4.1. Light Microscopy. A sample with $w_{PVME} = 0.50$ was dynamically cooled at 10 °C/min to −40 °C. From the calorimetric observations it could be concluded that at this temperature (almost) only the crystallization of free water takes place. Typical observations (nonpolarized light) are reported in Figure 10. Large spherulitic-like structures, which are completely opaque and not birefringent, are formed (Figure 9a,b, increasing time). Similar observations have been done in PVP/water and glycerol/water mixtures.[12] Once these structure are completely formed they become more transparent, showing the inside lamellar texture (Figure 9c, after 10 min). At the end of this growth, water has only partially crystallized. This was clearly illustrated by the parallel investigation by wide-angle and small-angle X-ray scattering discussed next.

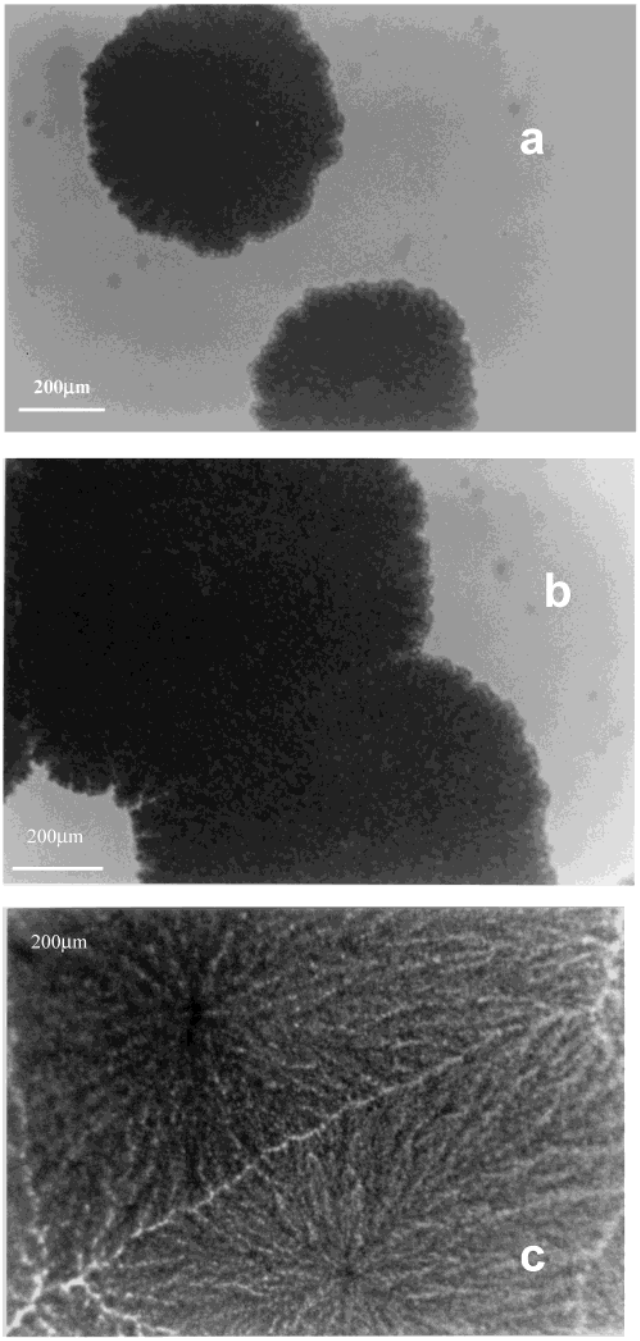

Figure 10. Optical microscopy observation of the formation of supramolecular structures during the formation of ice in a solution with $w_{PVME} = 0.50$ at −40 °C. Total time: 10 min.

3.4.2. WAXS and SAXS. The time dependence of the WAXS pattern at −40 °C with $w_{PVME} = 0.50$ is shown in Figure 11. After 1 min three maxima develop at $2\theta = 23.91°$, 24.3°, and 40.93°. Their intensity increases

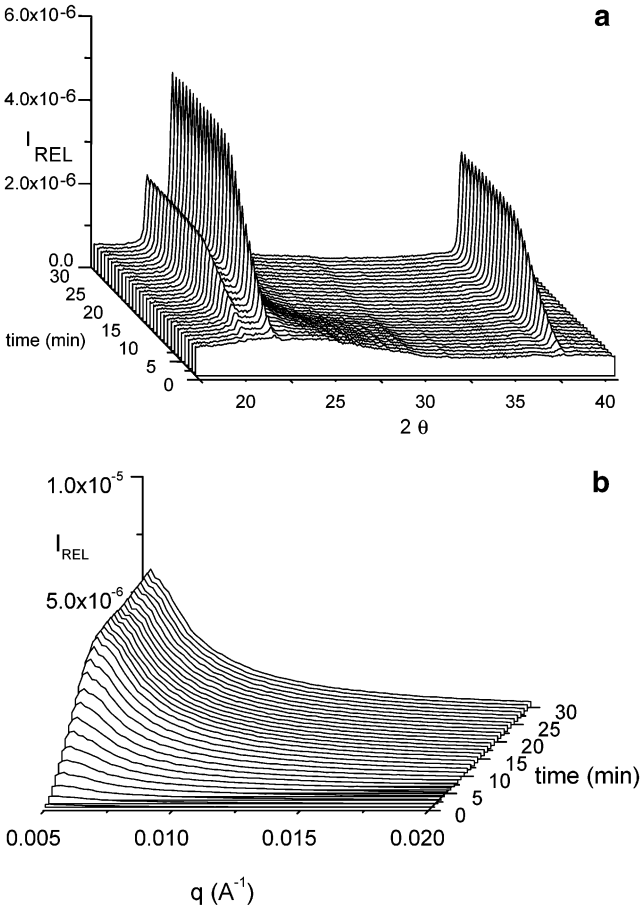

Figure 11. Time dependence of WAXS (a) and SAXS (b) patterns of a solution with $w_{PVME} = 0.50$ at −40 °C.

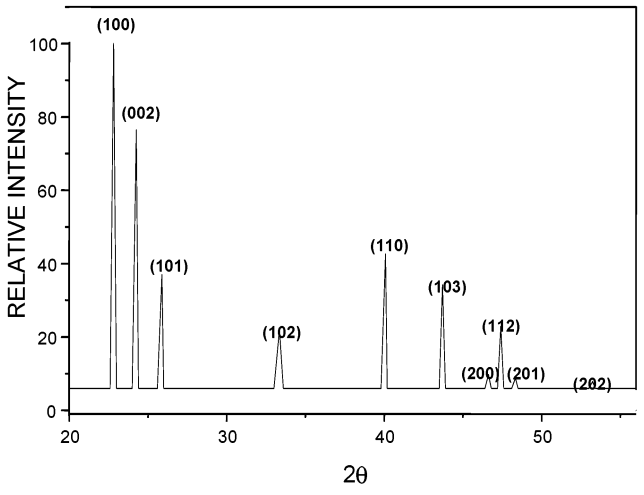

Figure 12. WAXS pattern of hexagonal ice.

until a plateau value is reached after about 14 min. These signals are characteristic for hexagonal ice and point to the presence of the (100), (002), and (110) diffraction planes. The signals at $2\theta = 26°$ and 33.88°, corresponding to the (101) and (102) planes, are not present as could be expected from the diffraction pattern of hexagonal ice, shown for comparison in Figure 12.

An important difference with the diffraction pattern of well-developed hexagonal ice is the difference in intensity ratio between the (100) and (002) planes. The most developed signal is that of the (002) plane while the opposite is normally observed. This reflects the preferential growth of the hexagonal ice crystals in one

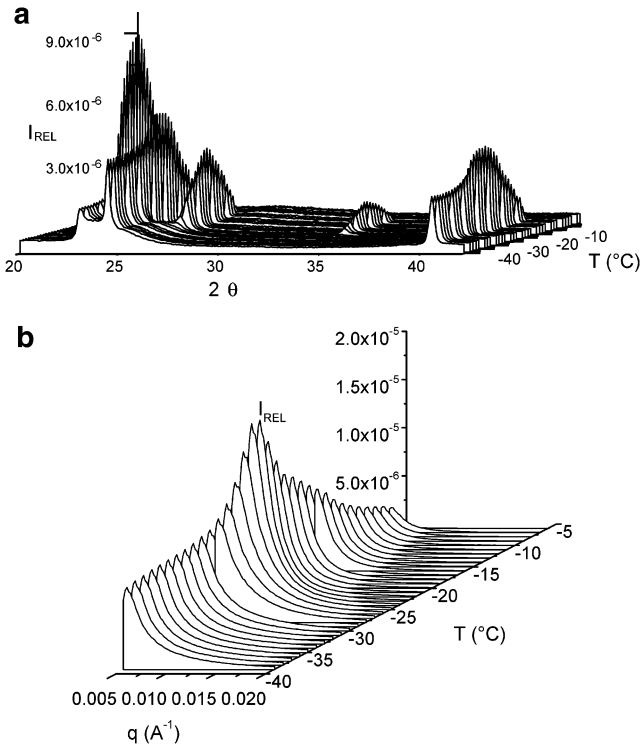

Figure 13. Changes in WAXS (a) and SAXS (b) patterns of a solution with $w_{PVME} = 0.50$ during heating at 1 °C/min from −40 °C to room temperature.

direction with a strongly reduced development in the other crystallographic directions. The simultaneously recorded SAXS pattern shows the development of a well-defined maximum. This transformation sets in after 1 min and ends after 14 min, paralleling the WAXS results.

It is also during this period that short-lived but intense spots appear in the 2-dimensional SAXS pattern. Collection of these spots over an extended time period a scattering pattern consisting of streaks is formed, in agreement with a plane hexagonal lattice structure in the mixture. This is in agreement with recent observations in PVP/water.[14,15]

Changes in the scattering and diffraction patterns take place on heating (Figure 13). In the WAXS region, the intensity of the patterns remains constant up to −35 °C, but at higher temperature an increase of the intensity takes place. The signal at $2\theta = 23.91°$ becomes now the most important as is observed with fully developed ice crystals. In addition at −28 °C, the signals at $2\theta = 26°$ and 33.88° appear. This change in the diffraction pattern points to an increase in the crystallinity and to the development of the ice crystals in other crystallographic directions. A decrease of the intensity sets in when −23 °C is reached, and no scattering is anymore observed when −6 °C is approached. An increase of the intensity and shift to lower q values, indicative of an improved structural contrast, followed by a decrease in intensity, due to melting of ice, is also observed in the SAXS signal.

3.4.3. Interpretation of the Morphological Data. The growth process of ice crystals can be understood in the following way. This is illustrated in Figure 14. Crystallization starts at a few nuclei. From these centra, fibrillar ice crystals develop in a preferential growth direction along the *c*-axis of the hexagonal ice crystals, resulting in a diffraction pattern with the highest

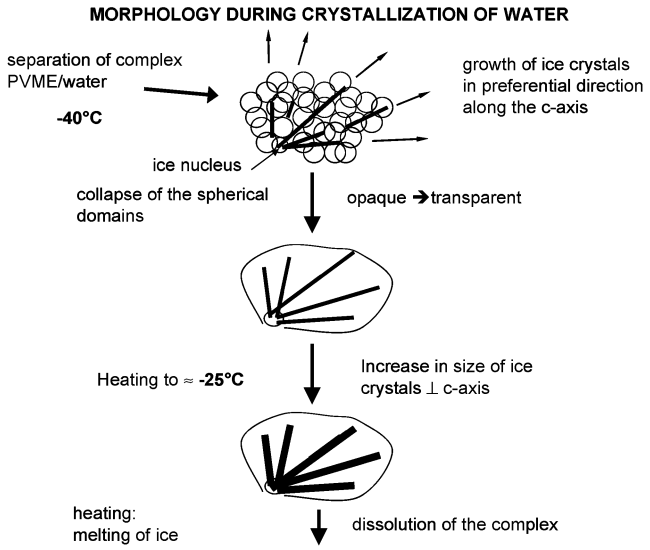

Figure 14. Schematic representation of the growth of ice crystals at −40 °C (w_{PVME} = 0.50).

intensity along the (002) plane. This crystallization separates droplets of highly concentrated polymer solution. These agglomerations of droplets make the system opaque and hide the fibrillar ice crystals. At the end of the process, these droplets coalesce, and the matrix around the ice crystals becomes transparent. On heating, crystallization of water is continuous so that ice crystals grow in other directions, resulting in a higher crystallinity and a development of larger crystals which is reflected in the expected ratio of peak intensities.

These observations further support earlier statements. At −40 °C and lower temperatures crystallization of water is limited, while in the temperature region −30 to −20 °C almost complete crystallization of water can take place.

3.5. Crystallization of Water in the High Concentration Range, $w_{PVME} > 0.61$. In previous sections it was stated that samples with $w_{PVME} > 0.61$ never show crystallization of water for the different crystallization conditions applied so far. To further investigate this behavior, the following experiment was carried out. A sample with w_{PVME} = 0.70 was brought in contact with water vapor at −50 °C in order to crystallize ice on the surface of the highly viscous solution. Then the sample was annealed at −35 °C as a function of time. The different stages in this annealing experiment are illustrated in Figure 15. During the annealing, ice crystals grow, starting at the solution−ice interface, throughout the solution up to almost complete transformation of the system into PVME and ice crystals. From these observations we can conclude that in the presence of ice crystals, which can act as nucleation sites, crystallization is possible also at higher concentrations.

4. Discussion and Conclusions

The reported data clearly indicate the significant influence of the experimental conditions on the crystallization and subsequent melting of water in the system PVME/water. The following conclusions can be drawn from the experimental data presented in this paper.

In agreement with previous reported results and for certain experimental conditions used in this study, the experimental results can be interpreted to give proof of the existence of a molecular complex between water and

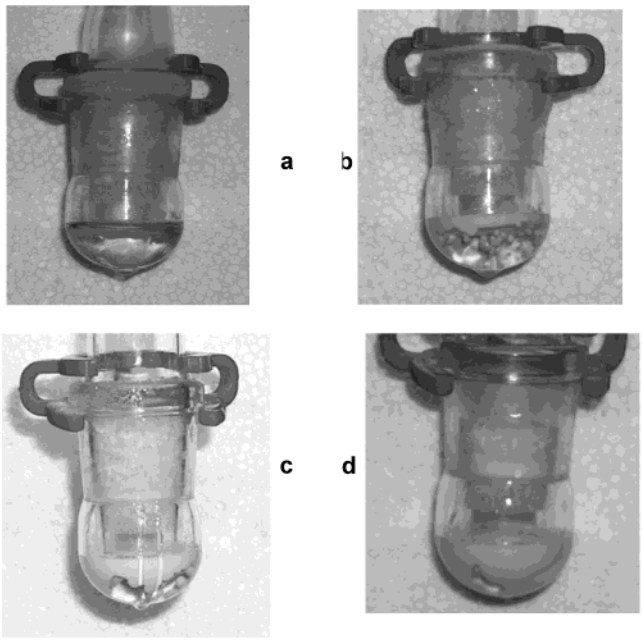

Figure 15. Crystallization of water from a solution with w_{PVME} = 0.70 induced by ice nuclei formed at its surface: (a) 6 h "etching" with ice crystals at −50 °C. Annealing at −35 °C for (b) 17, (c) 42, and (d) 186 h.

PVME in which two water molecules are bound to a polymer repeat unit. This conclusion is based on the following arguments:

For polymer concentrations $0 < w_{PVME} < 0.61$ isothermal treatments at lower temperature, say $T <$ −35 °C, or dynamic crystallization of water after quenching to very low temperature leads to only partial crystallization of water. This has been interpreted as the crystallization of "free water" and leaving the water bonded to the PVME chain in the PVME/water complex intact. The incomplete crystallization of water in the low-temperature region (−50 to −40 °C) is also seen in the WAXS and SAXS patterns.

For polymer concentrations $w_{PVME} > 0.61$ no crystallization of water is observed for "normal" crystallization conditions. The composition w_{PVME} = 0.61 coincides with the ratio of two water molecules per polymer repeating unit. For higher polymer concentrations all water molecules are complexed to the polymer chain and resist crystallization.

Related to this, the concentration dependence of the heat of melting ΔH_m observed under these crystallization conditions also supports the existence of the polymer/water complex. In fact, the extrapolation of experimental data of $\Delta H_m = 0$ at a nonzero water concentration is a classic method to determine the complex composition from thermodynamic data such as the heats of melting.[26] Hence, no melting (thus no crystallization) of water is observed for polymer concentrations $w_{PVME} > 0.61$.

Further indirect evidence for the existence of a molecular polymer/water complex and the composition of the complex is given by the change in the concentration dependence of the glass transition temperature of homogeneous polymer solutions obtained by deep quenches.

However, further experimental evidence presented in this study clearly demonstrates that the complex is thermodynamically unstable and is only observed under

certain kinetic conditions. This can be concluded from the following observations:

For polymer concentrations $0 < w_{PVME} < 0.61$ almost full crystallization of water can be realized by isothermal annealing in the temperature region −20 to −30 °C or slow cooling to low temperature. This is confirmed by data on the melting enthalpy of water, the shift in the absorption peaks in IR, and the volume change in dilatometric experiments. When crystallization is realized at not too low temperature and sufficient annealing time is allowed for, the crystallization does not stop at the composition of the complex but proceeds up to the point where the glass transition temperature of the polymer solution at the annealing of crystallization temperature is reached. A lower limit for the annealing temperature seems to be around −30 °C. Below this temperature the system becomes too close to the glass transition of the mixture during the crystallization of water, and full crystallization of water is no longer observed.

Consequently, the heats of melting determined for this type of crystallization/annealing experiments extrapolate to $\Delta H_m = 0$ at $w_{PVME} = 1$ instead of $w_{PVME} = 0.61$.

In the low-temperature region (−50 °C) the incomplete crystallization of water was confirmed by WAXS and SAXS experiments. However, when the samples are heated after this isothermal treatment, the crystallinity increases when a temperature around −30 °C is reached.

In the concentration range $w_{PVME} > 0.61$, which never resulted in crystallization of water for "normal" crystallization conditions, the crystallization of water can be realized provided the nucleation of water is facilitated. As realized in this paper, crystallization occurs if nucleation is provided by for example ice crystals, from which crystal growth can occur. Of course, this can only be realized as long as the barrier for crystal growth is still surmountable. That is, if sufficient undercooling is realized and the crystallization temperature is not too close to the glass transition temperature at these high polymer concentrations in which case kinetic aspect related to the high viscosity in the vicinity of the glass transition temperature will prevent crystal growth. It is anticipated that the crystallization under so-called "normal" crystallization conditions does not occur because the activation energy for nucleation is too large under the experimental conditions, and it is the nucleation that is arrested. However, as soon as nuclei are present, the crystal growth, which has lower activation energy, can still occur in the accessible experimental window between the melting point temperature and the glass transition temperature, which come closer and closer to each other at higher polymer concentrations. In the absence of ice, either deliberately introduced or formed by the crystallization of free water, the complex does not decompose. Further experiments to falsify or confirm this hypothesis are currently in progress.

Finally, it can be observed that IR spectroscopy is an elegant and powerful technique to investigate the changes in local environment in crystallizing systems, enabling us to determine in situ the polymer concentration in the polymer-rich phase that is left after crystallization of water.

Acknowledgment. The work was supported by the Bilateral (international) scientific and technological cooperation of the Ministry of the Flemish Community and the Ministry of Science and Technology of the People Republic of China (BIL01/06). The authors thank the Funds for Scientific Research Flanders (FWO) and IUAP5/03 (Belgian Program on Inter University Attraction Poles initiated by the Belgian State Prime Ministers office) for financial support. They are also indebted to the Flemish Institute for the promotion of Scientific-Technological Research in Industry (IWT) for a fellowship for (F.M.). We also thank the staff of DUBBLE, the Dutch−Belgian Beamline at the European Synchrotron Radiation Facility, Grenoble, France.

References and Notes

(1) Responsive gels: Volume transitions I and II; *Adv. Polym. Sci.* **2000**, *109* and *110*.
(2) *Water-Soluble Polymers*; Shalaby, S. W., McCormick, C. L., Butler, G. B., Eds.; ACS Symposium Series; American Chemical Society: Washington, DC, 1991; Vol. 467.
(3) Sato, H. *Adv. Polym. Sci.* **2000**, *109*, 207.
(4) Afroze, F.; Nies, E.; Berghmans, H. *J. Mol. Struct.* **2000**, *554*, 66.
(5) Moerkerke, R.; Meeussen, F.; Konigsveld, R.; Berghmans, H.; Mondelaers, W.; Schacht, E.; Dusek, K.; Solc, K. *Macromolecules* **1998**, *31*, 2223.
(6) Moerkerke, R.; Koningsveld, R.; Berghmans, R.; Dusek, K.; Solc, K. *Macromolecules* **1995**, *28*, 1103.
(7) Solc, K.; Dusek, K.; Koningsveld, R.; Berghmans, H. *Collect. Czech. Chem. Commun.* **1995**, *60*, 1661.
(8) Schäfer-Soenen, H.; Moerkerke, R.; Berghmans, H.; Koningsveld, R.; Dusek, K.; Solc, K. *Macromolecules* **1997**, *30*, 410.
(9) Moerkerke, R.; Koningsveld, R.; Nies, E.; Berghmans, H.; Dusek, K.; Solc, K. *Wiley Polym. Networks Group Rev. Ser.* **1998**, *1*, 463.
(10) Flory, P. J. *J. Chem. Phys.* **1942**, *9*, 660.
(11) Huggins, M. L. *J. Chem. Phys.* **1942**, *9*, 440.
(12) Franks, F. In *Water, a Comprehensive Treatise*; Franks, F., Ed.; Plenum Press: New York, 1982; Vol. 7, Chapter 3.
(13) MacKenzi, A. P.; Rasmussen, D. H. In *Water Structure at the Water-Polymer Interface*; Jellinek, H. H. G., Ed.; John Wiley: New York, 1972.
(14) De Dood, M. J. A.; Kalkman, J.; Strohhofer, C.; Michielsen, J.; Van der Elsken, J. *J. Phys. Chem. B* **2003**, *107*, 5906.
(15) Van der Elsken, J.; Bras, W.; Michielsen, J. C. F. *J. Appl. Crystallogr.* **2001**, *34*, 62.
(16) Meeussen, F. Ph.D. Thesis, Catholic University of Leuven, 2002.
(17) Meeussen, F.; Bauwens, Y.; Moerkerke, R.; Nies, E.; Berghmans, H. *Polymer* **2000**, *41*, 3737.
(18) Maeda, Y.; Higuchi, T.; Ikeda, I. *Langmuir* **2000**, *16*, 7503.
(19) Maeda, Y. *Langmuir* **2001**, *17*, 1737.
(20) Maeda, Y.; Nakamura, T.; Ikeda, I. *Macromolecules* **2002**, *35*, 217.
(21) Zhang, J. M.; Zhang, G. B.; Wang, J. J.; Lu, Y. L.; Shen, D. Y. *J. Polym. Sci., Part B: Polym. Phys.* **2002**, *40*, 2772.
(22) Zhang, J. M.; Teng, H.; Zhou, X.; Shen, D. Y. *Polym. Bull. (Berlin)* **2002**, *48*, 277.
(23) Norio, M.; Kiuji, G.; Tokuko, W. *J. Phys. Chem.* **1986**, *90*, 5420.
(24) Gabriel, A.; Dauvergne, F. *Nucl. Instrum. Methods* **1982**, *201*, 223.
(25) Zhukov, V.; Udo, F.; Marchena, O.; Hartjes, F. G.; Van den Berg, F. D.; Bras, W.; Vlieg, E. *Nucl. Instrum. Methods A* **1997**, *392*, 83.
(26) Buyse, K.; Berghmans, H. *Polymer* **2000**, *41*, 1045.

MA0303869